

Star Formation Rate of Eight Nearby Dwarf Galaxies within 85 Mpc Distance

P. Pangali, J. Malla, A. K. Jha, D. N. Chhatkuli and B. Aryal

Journal of Nepal Physical Society

Volume 9, Issue 1, June 2023

ISSN: 2392-473X (Print), 2738-9537 (Online)

Editor in Chief:

Dr. Hom Bahadur Baniya

Editorial Board Members:

Prof. Dr. Bhawani Datta Joshi

Dr. Sanju Shrestha

Dr. Niraj Dhital

Dr. Dinesh Acharya

Dr. Shashit Kumar Yadav

Dr. Rajesh Prakash Guragain

JNPS, 9 (1): 122-128 (2023)

DOI: <https://doi.org/10.3126/jnphysoc.v9i1.57749>

Published by:

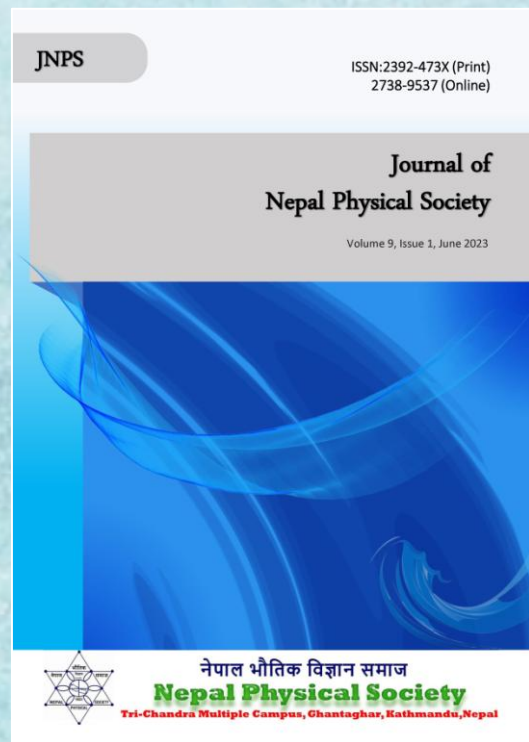
Nepal Physical Society

P.O. Box: 2934

Tri-Chandra Campus

Kathmandu, Nepal

Email: nps.editor@gmail.com





Star Formation Rate of Eight Nearby Dwarf Galaxies within 85 Mpc Distance

P. Pangali, J. Malla, A. K. Jha*, D. N. Chhatkuli and B. Aryal

Central Department of Physics, Tribhuvan University, Kirtipur, Kathmandu, Nepal

*Corresponding Email: ajay.jha@cdp.tu.edu.np / astroajay123@gmail.com

Received: 11th March, 2023; Revised: 26th June, 2023; Accepted: 30th June, 2023

ABSTRACT

This study examines the star formation rates (SFR) of eight dwarf galaxies, namely IC 700, MRK 0225, NGC 3440, NGC 5089, PGC 026162, PGC 051103, UM 158, and UM 454. The SFR estimators include the luminosities of the H alpha and [OII] emission lines, as well as the ultraviolet continuum. The data is obtained from GALEX and SDSS spectral observations. Of the eight galaxies, seven are classified as starburst dwarfs, while PGC 026162 is identified as a Seyfert galaxy. The highest H alpha SFR is observed in MRK 0225, measuring 0.30466 solar masses per year, whereas IC 0700 exhibits the lowest value of 0.00096 without accounting for extinction. However, upon correcting for extinction, the values become 0.84543 and 0.00177, respectively. In terms of OII SFR, MRK 0225 demonstrates the highest value of 0.32111, while IC 0700 displays the lowest at 0.00232. Additionally, MRK 0225 also exhibits the highest NUV SFR with a value of 0.19725, whereas IC 0700 shows the lowest NUV SFR at 0.06462. Upon applying the extinction correction, these values become 0.47936 and 0.10162, respectively. Analysis reveals that MRK 0225 and UM 158 have experienced recent increases in SFR, indicating a significant presence of newly formed stars. Conversely, UM 454 has maintained a relatively constant SFR for approximately 100 million years. Finally, NGC 3440, IC 700, NGC 5089, and PGC 051103 demonstrate a recent decline in SFR, suggesting a depletion of gaseous content available for star formation. The study also examines the line metallicity by assessing the ratio of NII to H alpha, identifying two galaxies, UM 158 and UM 454, with notably low line metallicity values of 8.11 and 8.13, respectively. Our samples also reveal a consistent trend: galaxies located at greater distances exhibit a notably higher rate of star formation. Overall, the findings indicate that these dwarf galaxies align with the trends observed in local-volume, star-forming galaxies.

Keywords: Dwarf galaxy, Emission line, Line metallicity, Star formation history, Star formation rate.

1. INTRODUCTION

Dwarf galaxies are the smallest and most abundant type of galaxy in the universe, with masses $\sim 10^8$ times those of the Sun [1]. Despite their small size, they are crucial for understanding galaxy evolution as they are thought to be building blocks for larger galaxies. One key aspect of dwarf galaxies is their star formation activity, which plays a crucial role in shaping their evolution. A study of the star formation rate of dwarf galaxies can provide some insights into the complex interplay between gas content, star formation activity, and other physical properties of galaxies [2].

Recent studies have suggested that dwarf galaxies have higher gas concentrations and are more active in forming stars than previously thought. However, their SFRs and star formation histories remain poorly understood. The estimation of SFR in dwarf galaxies is often challenging due to their faintness and the difficulty in measuring their properties accurately. Nevertheless, several methods have been proposed to estimate SFR in dwarf galaxies, such as the luminosities of various emission lines, the ultraviolet continuum, and infrared radiation. In this context, we have analyzed the SFRs of eight dwarf galaxies selected based on their high gas

concentrations and star-forming activity. We examined photometric and spectroscopic data to provide a comprehensive analysis of the SFR and line metallicity of these galaxies. This study sheds light on the SFR variability among dwarf galaxies and provides insights into their star formation histories, which can contribute to a better understanding of the evolution of galaxies [2].

This paper is organized as follows: Section 2 explains the methodology, followed by discussion in Section 3. Finally, a conclusion and future works are given in Section 4.

2. METHODS

To select the eight dwarf galaxies from the article "A catalog of merging dwarf galaxies in the local universe [1]", we utilized data available in Sky Server's EXPLORE THE UNIVERSE WITH THE SLOAN DIGITAL SKY SURVEY Data Release 17*, the High Energy Astrophysics Science Archive Research Center (HEASARC) at the NASA/GSFC Astrophysics Science Division, and Galaxy Evolution Explorer (Galex)**. We extracted the spectra of the chosen dwarf galaxies by entering the right ascension, declination, or cataloged name of each galaxy into SDSS DR17. These spectra were downloaded from the SDSS database.

To smooth the pattern of the detected galaxy spectra, we applied the cubic spline interpolation method throughout the project. We then plotted the characteristic peaks of strong emission or absorption lines using a Gaussian fit from the fit data of the galaxy spectra. This allowed us to obtain parameters such as the Gaussian center, area, FWHM, height of the Gaussian, continuum level, and more. To calculate the redshift of each galaxy, we used the strong emission lines in the spectra and analogous ones made in a lab. This allowed us to accurately determine the redshift of the galaxies in our sample.

$$SFR(H\alpha) (M_{\odot}yr^{-1}) = 10^{0.4A_{H\alpha}} \times 7.94 \times 10^{-42} L_{H\alpha}(erg/s) \dots\dots\dots (5)$$

$$SFR(H\alpha) (M_{\odot}yr^{-1}) = 10^{0.4A_{H\alpha}} \times 7.94 \times 10^{-42} \times Area \text{ of Gaussian Fit} \times 10^{-17} \times 4\pi d^2 \dots\dots\dots (6)$$

A semi-empirical approach given by Gallagher, Hunter & Bushouse (1989) using a sample of 75 blue galaxies and by Kennicutt (1992) from a sample of 90 normal and irregular galaxies

$$SFR(OII) (M_{\odot}yr^{-1}) = 1.4 \times 10^{-41} L_{[OII]}(erg/s) \dots\dots\dots (7)$$

* <https://skyserver.sdss.org/dr17/>

** <https://skyview.gsfc.nasa.gov/current/cgi/query.pl>

In this case λ_{obsv} represents the observed value wavelength of emission line with respect to the Gaussian fit and λ_{emit} represents the laboratory emitted value wavelength used corresponding to the particular line. The redshift (z) of the galaxy is given by the following formula:

$$z = \frac{\lambda_{obsv} - \lambda_{emit}}{\lambda_{emit}} \dots\dots\dots (1)$$

The radial velocity of the galaxy can be calculated using the simple relation, $V_r = c.z$, with $c = 299792.458$ km/s. From V_r , the distance of this galaxy can be calculated with the Hubble Law relation:

$$Distance(d) = V_r / H_o = \frac{c.z}{H_o} \times 10^6, \text{ in parsecs} \dots\dots\dots (2)$$

Here, Hubble constant, $H_o = 70$ km/s/Mpc and 1 parsec = 3.08568×10^{16} m.

The line ratio of $H\alpha$ to $H\beta$ i.e., Blamer decrement is given by, $c = H\alpha/H\beta = \frac{f_{H\alpha}}{f_{H\beta}}$ [3]. The theoretical value of c i.e., $c_o = 2.85$ using electron temperature of 10^4 K. And finally, extinction [3],

$$A(H\alpha) = A_{H\alpha} = 5.208 \times \log \left(\frac{1}{2.85} \frac{f_{H\alpha}}{f_{H\beta}} \right) \dots\dots\dots (3)$$

Using the value of observed flux $F(H\alpha)_{obs}$ and extinction in the equation [4],

$$A(H\alpha) = -2.5 \log (F(H\alpha)_{obs}/F(H\alpha)_{em}),$$

the emitted flux $F(H\alpha)_{em}$ can be calculated in $erg/s/cm^2/\text{\AA}$.

$$F(H\alpha)_{em} = 10^{A(H\alpha)/2.5} F(H\alpha)_{obs} \dots\dots\dots (4)$$

The star formation rate suggested by Kennicutt, 1998 from the techniques of $H\alpha$ luminosity measurement is [2, 3, 5]:

combining the $SFR(H\alpha)$ with the average $H\alpha/[O II] \lambda\lambda 3727/3729 \text{ \AA}$ ratio to estimate SFR from $[OII] \lambda\lambda 3727/3729 \text{ \AA}$ is given by [2, 3, 5]:

$$SFR(OII) (M_{\odot}yr^{-1}) = 1.4 \times 10^{-41} \times \text{Area of Gaussian Fit} \times 10^{-17} \times 4\pi d^2 \dots\dots\dots(8)$$

The UV SFRs can be obtained using GALEX Near UV (NUV ($\lambda_{\text{eff}} \sim 2310 \text{ \AA}$, 1771–2831 \AA)) photometric data [2],

$$SFR_{UV} (M_{\odot}yr^{-1}) = 1.08 \times 10^{-28} L_{UV} \times 10^{0.4A_{UV}} \quad (9)$$

$$SFR_{UV} (M_{\odot}yr^{-1}) = 36 \times 10^{-29} \times cnt \times 1.08 \times 10^{-28} \times 4\pi d^2 \times F_{avg} \times 10^{0.4A_{UV}} \dots\dots\dots(10)$$

Where, d is in centimeter and F_{avg} as average value of flux density after background correction just we get after processing in aladin software. Also $A_{UV} = 0.87A(H\alpha)$ refers to the extinction in this case [3].

From the emission line metallicity using the calibration provided by Marino et al. (2013) i.e., $12 + \log(O/H) = 8.743 + 0.462 \times \log(NII/H\alpha)$, calculated from line ratio between NII ($\lambda = 6585.6\text{\AA}$) and H α [4, 6]. The line ratio NII/H α is the ratio of the gaussian area of the emission lines.

Since, the Gaussian distribution function used throughout this dissertation is,

$$f(x) = Ae^{-\frac{(x-\mu)^2}{\sigma^2}} \dots\dots\dots(11)$$

Area of the function is given by,

$$\int_{-\infty}^{\infty} Ae^{-\frac{(x-\mu)^2}{\sigma^2}} = A\sqrt{\pi\sigma^2}.$$

For some real constants A , μ and σ .

The SFR of the sample galaxies indicated by OII and H alpha emission lines represents recent star

here L_{UV} is the observed UV luminosity in units of erg/s/Hz and A_{UV} is the dust attenuation. Now the star formation rate considering total count of pixels of the galaxy is given by [2],

formation ~ 10 Myr but NUV SFR ~ 100 Myr is slightly different than previous [3].

The Blue-band magnitudes are derived from the SDSS g-band and r-band magnitudes using the following equation [1],

$$m_b = g + 0.3130 \times (g - r) + 0.2271 \dots\dots\dots(12)$$

To find the blue absolute magnitude M_b , we need to know its distance and blue apparent magnitude m_b . The magnitude–distance formula relates the apparent magnitude m_b , absolute magnitude M_b , and the distance d in parsecs as:

$$m_b - M_b = -5 + 5\log_{10}(d) \dots\dots\dots(13)$$

The quantity $m_b - M_b$ is called the distance modulus. It indicates the amount by which distance has dimmed the starlight.

3. RESULTS AND DISCUSSION

The images of these sample galaxies downloaded from SDSS skyserver dr17 are shown below:

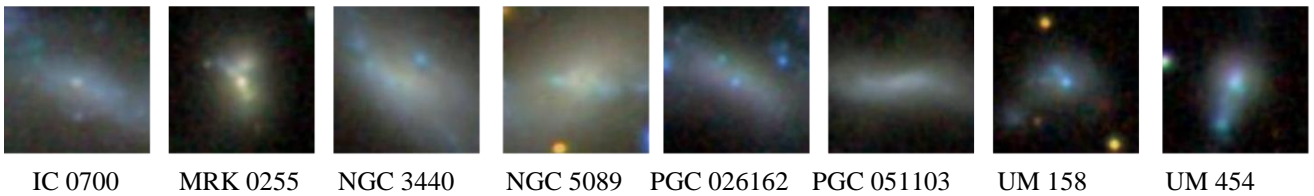


Fig. 1: Images of sample Dwarf Galaxies IC 0700, MRK 0255, NGC 3440, NGC 5089, PGC 026162, PGC 051103, UM 158, and UM 454 taken from SDSS.

The most frequent star formation rate (SFR) estimator is Balmer emission lines, especially the H α line, a direct star formation probe for total ionizing flux. Therefore, it is the most popular and accurate method used to calculate the SFR. Forbidden lines such as the [O II] ($\lambda\lambda 3727, 3729$) is also used for SFR estimation, but this method is affected by metallicity and reddening of the galaxy. Finally, the Ultraviolet (UV) continuum flux can

also give a measure for the SFR. Each method gives different information about the stellar populations in the galaxies, measures slightly different aspects of SFRs and have different strengths and weaknesses. The emission lines and the UV continuum are also sensitive to different stellar masses with emission lines being more sensitive to lower mass stars.

Table: Star formation rate of sample dwarf galaxies using H alpha, OII, and NUV luminosities, extinction correction and Line Metallicity.

Galaxies	Redshift (z)	SFR (H α) ($M_{\odot}\text{yr}^{-1}$)	SFR (OII) ($M_{\odot}\text{yr}^{-1}$)	Extinction A(H α)	Extinction Corrected H α SFR ($M_{\odot}\text{yr}^{-1}$)	NUV SFR ($M_{\odot}\text{yr}^{-1}$)	Extinction Corrected NUV SFR ($M_{\odot}\text{yr}^{-1}$)	Line Metallicity (12+ log(O/H))
IC 0700	0.00469	0.00096	0.00232	0.66263	0.00177	0.06462	0.10989	8.37766
NGC 3440	0.0064	0.00601	0.01562	0.23334	0.00745	0.1183	0.14262	8.37365
NGC 5089	0.00707	0.01267	0.01918	1.07652	0.03416	0.17189	0.40727	8.41362
PGC 026162	0.00872	0.0034	0.0392	-4.45048	-	-	-	8.56949
UM 454	0.01304	0.11247	-	0.09764	0.12306	0.16789	0.18155	8.13407
UM 158	0.01457	0.13268	-	0.35116	0.18335	0.0767	0.10162	8.10883
PGC 051103	0.01491	0.05699	0.07125	0.99582	0.14259	0.15057	0.33441	8.24407
MRK 0225	0.01967	0.30466	0.32111	1.10817	0.84543	0.19725	0.47936	8.36228

Finally, we compare the Star Formation Rate of Galaxies with their Line Metallicity to study whether there is any relation between Metallicity and Star Formation Rate of these Galaxies. But the figure makes it difficult to extract any exact relationship between the line metallicity and the rate of star formation of the galaxies. The relation between metallicity and SFR is quite random for H

alpha and OII, but extinction-corrected NUV SFR shows some dependency on metallicity. With the increase in extinction-corrected NUV SFR, the line metallicity of the galaxy also increases. As we can see from all of the graphical relationships that SFR is generally increasing with distance throughout our samples. This implies that the farthest galaxies have a higher rate of star formation within our samples.

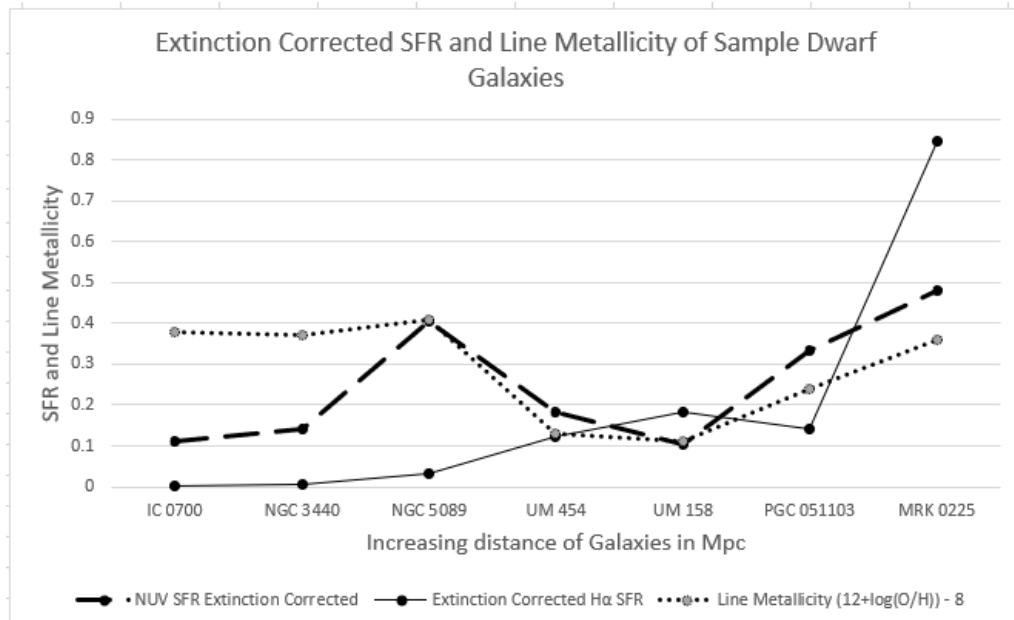


Fig. 2: Interpretation of line metallicity with the Extinction corrected SFR of different indicators i.e., SFR vs Line Metallicity - 8. Comparison for H alpha and NUV star formation rate. Star formation rate is in unit of solar mass per year and line metallicity - 8 is in dex.

Finally, to study the star formation history of these galaxies, we compare the star formation rate calculated using these three different approaches by

considering the fact that H alpha SFR and O II SFR indicators are the sign of recent star formation ~ 10Myr and NUV SFR indicator for ~100Myr. Star

Star Formation Rate of Eight Nearby Dwarf Galaxies within 85 Mpc Distance

formation rate of MRK 0225, UM 158 has shown recent increase and NGC 3440, UM 454, IC 700,

NGC 5089, PGC 051103 show recent decrease in SFR which are shown in figure below:

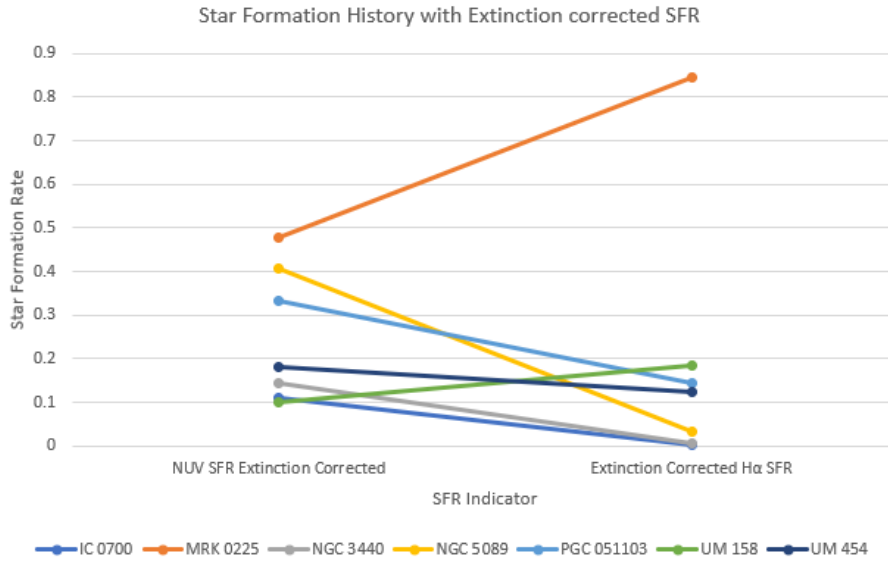


Fig. 3: Star formation history of sample galaxies IC 700, MRK 0225, NGC 3440, NGC 5089, PGC 051103, UM 158 and UM 454. Star formation rate is in the unit of solar mass per year and H alpha SFR is the sign of recent star formation ~ 10Myr and NUV SFR indicator for ~100Myr.

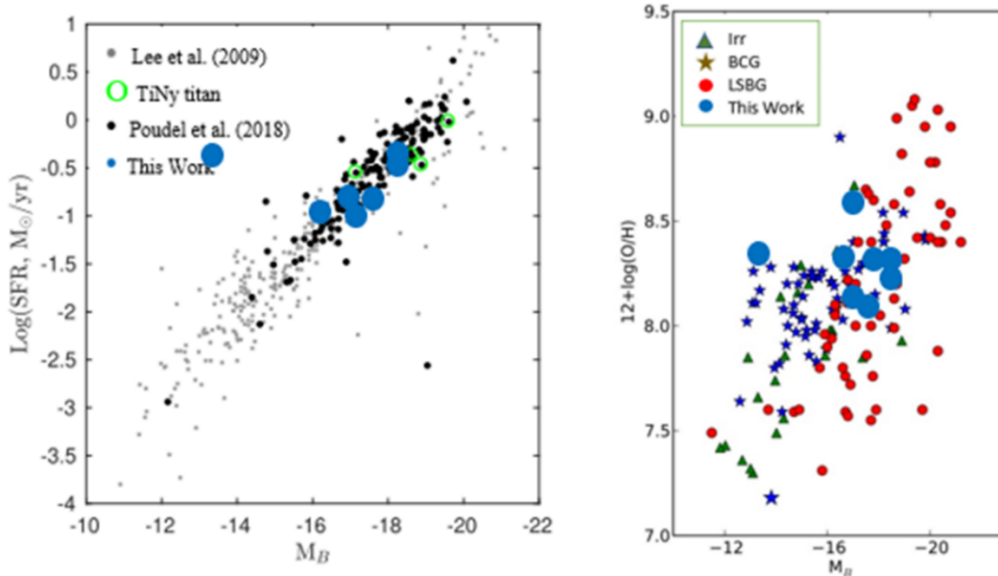


Fig. 4: (a) Comparison of Extinction Corrected UV Star formation rate vs. blue-band absolute magnitude of our sample galaxies with Lee et al. (2009) and Poudel et al. (2018) (left) (b) comparison of emission line metallicity with previous findings (right) [Image source: Bergvall].

A large number of studies regarding star formation rate of the dwarf galaxies had performed in the past by different researchers. For comparison of our study with previous results, we used the data from Poudel et al. (2018) and Lee et al. (2009), who studied the UV-derived SFRs. Figure 4 illustrates the relation between the B-band absolute magnitude

and the logarithm of the extinction-corrected SFR. The emission line metallicity obtained for the selected dwarf galaxies has been compared with the findings of Bergvall [6]. From this figure, it is clear that these dwarf galaxies do not differ from the trend established by local-volume, star-forming galaxies.

4. CONCLUSIONS

After the study of these sample dwarf galaxies using SDSS DR17 and Galex database, we conclude our result as follows.

(a) Emission Lines: The most common emission lines are 3727.092 [OII] (present in all but data unavailable for UM 158, UM 454), 3729.875 [OII] (present in all but data unavailable for UM 158, UM 454), 3868.76 [Ne III] (absent in IC 0700), 3967.47 [Ne III] (absent in IC 0700, NGC 5089), 4102.89 H δ , 4341.68 H γ , 4364.436 [O III] (only present in UM 158, UM 454 and PGC 026162), 4862.68 H β , 4960.295 [O III], 5008.24 [O III], 5875.624 He I, 6302.046 [O I], 6365.536 [O I] (only present in UM 158, UM 454 and MRK 0225), 6549.86 [N II], 6564.61 H α , 6585.27 [N II], 6718.29 [S II] (absent in NGC 3440), 6732.67 [S II], and 7135.79 [Ar III]. Out of these emission/absorption lines in the spectra of the galaxy, emission lines dominate the spectrum of all these galaxies.

(b) Classification of galaxies: Out of the 8 sample dwarf galaxies we classified 7 as starburst galaxies with line ratio (H α >> [N II] λ 6585 Å) but PGC 026162 as Seyfert galaxy with H α /2.5 \leq [N II] (λ 6585 Å) and [O III] (λ 5008 Å) >> H β .

(c) Star Formation Rate with H α Line: The H α line is an indication of hot young ionizing stars, thus galaxy which has high H α SFR means it is full of newly formed ionizing stars. The MRK 0225 has highest star formation rate of 0.30466 (extinction corrected \sim 0.84543) $M_{\odot}yr^{-1}$ while IC 0700 has lowest value of 0.00096 (extinction corrected \sim 0.00177) $M_{\odot}yr^{-1}$.

(d) Star Formation Rate with OII Line: Out of the 8 sample dwarf galaxies, OII lines data are available for only six. The OII SFR is highest for MRK 0225 with 0.32111 $M_{\odot}yr^{-1}$ and lowest for IC 0700 with 0.00232 $M_{\odot}yr^{-1}$.

(e) Star Formation Rate with NUV Band: The UV spectrum is characteristics of the continuum emission from hot young massive stellar clusters. Out of the 8 samples (except PGC 026162), MRK 0225 has highest SFR in NUV with the value of 0.19725 (extinction corrected \sim 0.47936) $M_{\odot}yr^{-1}$ and IC 0700 has lowest value of NUV SFR with the value of 0.06462 $M_{\odot}yr^{-1}$.

(f) Star Formation History: Star formation rate of MRK 0225, UM 158 has shown recent increase making them rich in recently formed stars, NGC 3440, UM 454, IC 700, NGC 5089, PGC 051103 show recent decrease in SFR i.e., all of the stars are

evolved and there remains less gaseous contents (i.e., hydrogen, helium) to form new stars.

(g) Line Metallicity: The value of line metallicity (12+log(O/H)) of galaxies ranges from 8.10883 for UM 158 to 8.56949 for PGC 026162.

(h) Comparison of Extinction Corrected UV Star formation rate vs. blue-band absolute magnitude of our sample galaxies with Lee et al. (2009) and Poudel et al. (2018) and comparison of emission line metallicity with previous findings i.e., Bergvall shows that these dwarf galaxies do not differ from the trend established by local-volume, star-forming galaxies.

Continuation to the Conclusion

Throughout this project, we studied the general characteristics of our sample dwarf galaxies of the local universe, which includes redshift, distance, star formation rate, star formation history, metallicity etc. but there are still lot of factors that can influence the observed properties. Some of them are galaxy merger, dark matter contents, kinematics, magnetic fields etc., they affect the evolution of galaxies and ultimate fate of the stellar evolution. We have ignored a lot of things during the study through data collections to the analysis and interpretation. A lot of things we haven't included in this study such as absorption lines of spectra (clue to the stellar properties), and we haven't covered whole electromagnetic spectrum, there might be a lot of errors in analysis and interpretations. Therefore, further research and analysis are required to clear the overall practical or theoretical understanding.

AUTHOR CONTRIBUTIONS

Whole calculation was done by first author. The second, third, and fourth authors crossed checked the calculations and suggested the nature of the plots. The last author provides the concept behind the work, also contributed in the discussion part.

ACKNOWLEDGEMENTS

We would like to show our appreciation to all the professors, seniors, and writers of the publications and resources (such as the SDSS/GALEX team) that we used throughout our project, whether or not they were personally involved.

REFERENCES

This research report is mainly based on the following resources:

- [1] Paudel, S.; Smith, R.; Yoon, S. J.; Calderón-Castillo, P. and Duc, P. A. A catalog of merging dwarf galaxies in the local universe. *The Astrophysical Journal Supplement Series.*, **237** (2): 36 (2018).
- [2] Harris, K. A. The Cluster and Large-Scale Environments of Quasars at $z < 0.9$. *arXiv preprint arXiv:1201.5746* (2012).
- [3] Gilbank, D. G.; Baldry, I. K.; Balogh, M. L.; Glazebrook, K. and Bower, R. G. The local star formation rate density: assessing calibrations using [O ii], H α and UV luminosities. *Monthly Notices of the Royal Astronomical Society*, **405** (4): 2594-2614 (2010).
- [4] Chhatkuli, D. N.; Paudel, S. and Aryal, B. Study of star formation rate and metallicity of an interacting dwarf galaxy NGC 2604. *Journal of Institute of Science and Technology*, **25** (2): 55-60 (2020).
- [5] Rosa-González, D., Terlevich, E. and Terlevich, R. An empirical calibration of star formation rate estimators. *Monthly Notices of the Royal Astronomical Society*, **332** (2): 283-295 (2002).
- [6] Gautam, S. P.; Silwal, A.; Sedain, A. and Aryal, B. Star Formation Rate of the Low Redshift Dwarf Galaxies J080947. 50+ 213717.2 and J151839. 94+ 220514.4. *Journal of Nepal Physical Society*, **7** (1): 18-24 (2021).
- [7] Arny, T. and Schneider, S. E. Explorations: Introduction to astronomy. *McGraw Hill Education* (2017).
- [8] Zezas, A. and Buat, V. (Eds.). Star-Formation Rates of Galaxies (Cambridge Astrophysics). *Cambridge: Cambridge University Press* (2021).
- [9] McConnachie, A. W. The observed properties of dwarf galaxies in and around the Local Group. *The Astronomical Journal*, **144** (1): 4 (2012).
- [10] Herrmann, K. A.; Hunter, D. A.; Zhang, H. X. and Elmegreen, B. G. Mass-to-Light versus Color Relations for Dwarf Irregular Galaxies. *The Astronomical Journal*, **152** (6): 177 (2016).
- [11] Roychowdhury, S.; Chengalur, J. N.; Karachentsev, I. D. and Kaisina, E. I. The intrinsic shapes of dwarf irregular galaxies. *Monthly Notices of the Royal Astronomical Society: Letters*, **436** (1): L104-L108 (2013).
- [12] Pflamm-Altenburg, J.; Weidner, C. and Kroupa, P. Converting H α luminosities into star formation rates. *The Astrophysical Journal*, **671** (2): 1550 (2007).
- [13] Falcón-Barroso, J. and Knapen, J. H. (Eds.). Secular evolution of galaxies (Vol. 23). *Cambridge University Press* (2012).
- [14] Vincoletto, L.; Matteucci, F.; Calura, F.; Silva, L. and Granato, G. Cosmic star formation rate: a theoretical approach. *Monthly Notices of the Royal Astronomical Society*, **421** (4): 3116-3126 (2012).
- [15] Almeida, J. S.; Terlevich, R.; Terlevich, E.; Fernandes, R. C. and Morales-Luis, A. B. Qualitative interpretation of galaxy spectra. *The Astrophysical Journal*, **756** (2): 163 (2012).
- [16] Kennicutt Jr, R. C.; Tamblyn, P. and Congdon, C. E. Past and future star formation in disk galaxies. *The Astrophysical Journal*, **435**: 22-36 (1994).
- [17] De Souza, A. A.; Martins, L. P.; Rodríguez-Ardila, A. and Fraga, L. Star Formation Rate Distribution in the Galaxy NGC 1232. *The Astronomical Journal*, **155** (6): 234 (2018).
- [18] Zhuang, M. Y. and Ho, L. C. Recalibration of [O ii] $\lambda 3727$ as a star formation rate estimator for active and inactive galaxies. *The Astrophysical Journal*, **882** (2): 89 (2019).
- [19] Lee, E. J.; Chang, P. and Murray, N. Time-varying Dynamical Star Formation Rate. *The Astrophysical Journal*, **800** (1): 49 (2015).
- [20] Hennebelle, P. and Chabrier, G. Analytical theory for the initial mass function. III. Time dependence and star formation rate. *The Astrophysical Journal*, **770** (2): 150 (2013).
- [21] Calzetti, D. Star formation rate indicators. *Secular Evolution of Galaxies*, **419**:... (2013).
- [22] Bertone, G. and Hooper, D. History of dark matter. *Reviews of Modern Physics*, **90** (4): 045002 (2018).
- [23] Kewley, L. J.; Nicholls, D. C. and Sutherland, R. S. Understanding galaxy evolution through emission lines. *Annual Review of Astronomy and Astrophysics*, **57**: 511-570 (2019).